

2006

Semi-Empirical 3D Rectangular Channel Air Flow Heat Transfer and Friction Factor Correlations

Ian E. Davidson

University of Illinois at Urbana-Champaign

Clark W. Bullard

University of Illinois at Urbana-Champaign

Follow this and additional works at: <http://docs.lib.purdue.edu/iracc>

Davidson, Ian E. and Bullard, Clark W., "Semi-Empirical 3D Rectangular Channel Air Flow Heat Transfer and Friction Factor Correlations" (2006). *International Refrigeration and Air Conditioning Conference*. Paper 751.
<http://docs.lib.purdue.edu/iracc/751>

This document has been made available through Purdue e-Pubs, a service of the Purdue University Libraries. Please contact epubs@purdue.edu for additional information.

Complete proceedings may be acquired in print and on CD-ROM directly from the Ray W. Herrick Laboratories at <https://engineering.purdue.edu/Herrick/Events/orderlit.html>

Semi-empirical 3D Rectangular Channel Air Flow Heat Transfer and Friction Factor Correlations

Ian E. Davidson¹, Clark W. Bullard^{2*}

¹University of Illinois Air Conditioning & Refrigeration Center
Urbana IL USA
+1 217 265 5308, +1 217 333 1942, bullard@uiuc.edu

²University of Illinois Air Conditioning & Refrigeration Center
Urbana IL USA
+1 217 333 7734, +1 217 333 1942, idavidso@uiuc.edu

ABSTRACT

This paper presents correlations for heat transfer and friction coefficients for combined entry region airflow in 3D rectangular channel as functions of channel depth, Reynolds number, hydraulic diameter, and channel aspect ratio. The correlations were designed to approach known physical limits as the channel aspect ratio and channel depth approach zero, and as the flow becomes fully developed. The curve fits were constructed by bridging continuously between these well known analytical and numerical results for 2D and 3D channels. The RMS value of the curve fits were 1.5 and 2.7% for heat transfer coefficient and friction factor, respectively. These physically-based correlations were created to be applied to the design and analysis of flat tube heat exchanger concepts in parts of the parameter space that lie outside the range of published empirical correlations.

1. INTRODUCTION

Microchannel heat exchangers are used widely for automotive a/c condensers and other applications where compactness is important. Their flat multiport tubes contribute to low air-side pressure drop and substantially increase refrigerant-side area, compared to the round tubes used in other applications. Recently, however, demands for increased efficiency in stationary a/c applications have led to increased outdoor air flow requirements to provide a larger heat sink. For this and other reasons, flat tube heat exchangers are now being considered for a wider range of applications where weight and flow depth are not as highly constrained as in mobile applications, and where air-side pressure drop is a more important consideration.

Unfortunately the empirical correlations developed for heat transfer and pressure drop on the air side of microchannel heat exchangers (Wang *et al.* 1999) are limited to the louvered fins, small fin pitch, short flow lengths and high face velocities typical of automotive applications. Such heat transfer and pressure drop correlations are generally accurate within $\pm 15\%$. On the other hand, flat-tube heat exchangers optimized for stationary heat pump applications may need plain fins to prevent condensate bridging and frost fouling, and to facilitate drainage of condensate and melt water. Since existing correlations are empirical, they cannot be extrapolated.

This paper develops air-side heat transfer and Darcy friction factor correlations that bridge – with a continuous function – the full range of rectangular channel hydraulic diameters, aspect ratios, flow lengths and laminar Reynolds numbers. It is suitable for use with optimization algorithms that cannot tolerate discontinuities as flow regimes change or geometric parameters approach 2D limits.

In order to be truly robust, a correlation must provide accurate predictions for any configuration. This was attempted by Muzychka and Yovanovich (2004). They developed a correlation for heat transfer in non-circular ducts of various shapes and sizes. The accuracy reported for this correlation is: “ $\pm 15\%$ for most non-circular ducts and channels.” Stephan (1959) addressed heat transfer in developing flow of a 2D duct, while Shah and London (1978) developed a correlation for friction factor. These correlations were based on numerical and analytical solutions and apply to any depth. To include the effect of channel aspect ratio, Shah and London (1978) also developed empirical

correlations for Nusselt number and friction factor in fully developed rectangular channels. These correlations were reported to be accurate within $\pm 0.05\%$ and 0.1% respectively.

2. METHODOLOGY

Existing correlations for rectangular channels are expressed in terms of two nondimensional geometric parameters, aspect ratio and flow depth. Two dimensional channel heat transfer and friction factor correlations are expressed as a function of non-dimensional depth, which is the flow length or heat exchanger depth (x^* for heat transfer and x_+ for friction factor, differing only due to the dependence of heat transfer on the Prandtl number) for simultaneously developing flow. For rectangular channels the aspect ratio $0 \leq \alpha \leq 1$ is the quotient of channel width over channel height.

The 3D correlations introduced here were constrained to approach three physically known limits: leading edge flow, fully developed flow, and a developing 2D duct (aspect ratio of zero) flow. Table 1 shows the scope of the 3D channel airflow heat transfer correlation with Nusselt numbers tabulated by Wibulswas and Stephan for varying aspect ratio and x^* with the three imposed physical limits. The same physical limits apply for friction factor.

Table 1. Wibulswas' numerical results, limiting cases and gaps

$1/x^*$	α					small	0 (Stephan)	$h_{Stephan}/h_{plate}$
	1	0.5	1/3	0.25	1/6			
	Fully developed							
10	3.75	4.2	4.67	5.11	5.72		7.839	3.54
20	4.39	4.79	5.17	5.56	6.13		8.143	2.6
30	4.88	5.23	5.6	5.93	6.47		8.443	2.2
40	5.27	5.61	5.96	6.27	6.78		8.734	1.972
50	5.63	5.95	6.28	6.61	7.07		9.017	1.821
60	5.95	6.27	6.6	6.9	7.35		9.292	1.713
80	6.57	6.88	7.17	7.47	7.9		9.823	1.568
100	7.1	7.42	7.7	7.98	8.38		10.33	1.475
120	7.61	7.91	8.18	8.48	8.85		10.81	1.409
140	8.06	8.37	8.66	8.93	9.28		11.28	1.361
160	8.5	8.8	9.1	9.36	9.72		11.72	1.323
180	8.91	9.2	9.5	9.77	10.12		12.15	1.294
200	9.3	9.6	9.91	10.18	10.51		12.57	1.269
220	9.7	10	10.3	10.58	10.9		12.98	1.249
2115	32.2	Flat Plate				32.2	34.24	1.063
6667	57.2					57.2	59.83	1.046

The upper limit of Graetz number ($1/x^* = 6667$) was chosen arbitrarily to serve as the lower limit on depth for the curve fit developed here. At the maximum laminar Reynolds number (2000) this corresponds to a hydraulic diameter to length ratio of 4.6, an extreme case lying outside the range of practical heat exchanger designs, at which the heat transfer coefficient was assumed to approach the flat plate limit. A similar table showing the same physical bounds was constructed for friction factor, but is not shown here for brevity.

Both the Nusselt Number and Darcy friction factor correlations were designed using the functional forms of the 2D duct correlations as the base cases. The nondimensional flow depths for heat transfer and friction factor, x^* and x_+ , are defined below in Equations 1 and 2. The 2D semi-analytical solutions for heat transfer and Darcy friction factor appear below as equations 3 and 4, respectively. The length scale used in the Reynolds number is the hydraulic diameter, which is equal to twice the duct height in the 2D case.

$$x^* = \frac{x}{D_h \cdot \text{Re}_{D_h} \cdot \text{Pr}} \tag{1}$$

$$x^+ = \frac{x}{D_h \cdot \text{Re}_{D_h}} \tag{2}$$

$$Nu_{2D} = 7.55 + \frac{0.024 \cdot x^{*-1.14}}{1 + 0.0358 \cdot \text{Pr}^{0.17} \cdot x^{*-0.64}} \tag{3}$$

$$f_{2D} = \frac{4}{\text{Re}_{D_h}} \cdot \left[\frac{3.44}{(x^+)^{1/2}} + \frac{24 + \frac{0.674}{4 \cdot x^+} - \frac{3.44}{(x^+)^{1/2}}}{1 + 0.000029 \cdot (x^+)^{-2}} \right] \tag{4}$$

These 2D expressions (Equations 3 and 4) were then modified to include dependence on channel aspect ratio, and to approach the known analytical limits of fully developed 3D channel flow and very short depth. For very short depth the flow was forced to approach that of a flat plate, neglecting perpendicular boundary layer interactions at the channel corners, thus neglecting all aspect ratio dependency at the leading edge. In fully developed channel flow of fixed aspect ratio, the Nusselt number and the product of friction factor and Reynolds number are known functions of the aspect ratio alone, as shown in Equations 5 and 6 below (Shah and London, 1978)..

$$Nu_{FD,rect} = 7.541 \cdot (1 - 2.61\alpha + 4.97\alpha^2 - 5.119\alpha^3 + 2.702\alpha^4 - 0.548\alpha^5) \tag{5}$$

$$f_{FD,rect} \cdot \text{Re}_{D_h} = 4 \cdot [24(1 - 1.3553\alpha + 4.97\alpha^2 - 5.119\alpha^3 + 2.702\alpha^4 - 0.548\alpha^5)] \tag{6}$$

Inside these three physical limits, tabular data from Wibulswas (1966) and Curr *et al.* (1972) for Nusselt Number and friction factor was bridged with an 8-parameter curve fit using least squares approach. The curve fits were weighted in an attempt to achieve a uniform distribution of accuracy. The power law dependence on aspect ratio yielded the best match to the results of Wibulswas (1966) and Curr *et al.* (1972). The 3D channel heat transfer correlation constructed using Wibulswas' (1966) results is discussed first.

3. 3D CHANNEL HEAT TRANSFER

Equation 7 shows how Stephan's expression for 2D flow was first modified to account for aspect ratio by multiplying the first term (7.55 for fully developed flow) by the polynomial correction factor developed by Shah and London (1978). The next step was to add 8 empirical parameters to the second term to capture the effects of aspect ratio in the developing flow regime.

$$Nu_{3D} = 7.55 \cdot (1 - 2.61\alpha + 4.97\alpha^2 - 5.119\alpha^3 + 2.702\alpha^4 - 0.548\alpha^5) + \frac{(0.024 + A_1\alpha^{A_2}) \cdot x^{*(-1.14 + B_1\alpha^{B_2})}}{1 + (0.03393 + C_1\alpha^{C_2}) \cdot x^{*(-0.64 + D_1\alpha^{D_2})}} \tag{7}$$

where

$A_1 = 0.247$	$A_2 = 1.049$	$B_1 = -0.1678$	$B_2 = 0.2109$
$C_1 = 0.987$	$C_2 = 0.8556$	$D_1 = -0.06201$	$D_2 = 1.211$

The functional form of this expression for 3D channel flow heat transfer was designed to reduce to the Stephan correlation when an $\alpha \rightarrow 0$. Similarly, it reduces to the fully developed rectangular solution (a function of aspect ratio alone) when the nondimensional depth x^* becomes large. Wibulswas (1966) presented 70 numerical results for Nusselt number as a function channel aspect ratio $1 < \alpha < 1/6$ and nondimensional depth $10 < 1/x^* < 220$.. The

curve fit used this data to give the 3D channel flow correlation the ability to predict heat transfer in between the channel geometric limits. Wibulswas' (1966) tabular data was reported to be accurate within a few percent when compared to experimental data for Graetz Numbers ($1/x^*$) less than 70. At larger Graetz numbers (short channels) the influence of the leading edge analytical bound shown in Table 1 is expected to improve the accuracy of the 3D channel heat transfer expression, but only up to the lower limit of the curve fit ($x^* = 1/6667$).

Figure 1 shows how the Stephan and 3D channel flow heat transfer coefficients vary with flow depth and approach the flat plate solution as $x^* \rightarrow 0$. Reducing x^* by decreasing heat exchanger depth has the same effect on heat transfer as increasing hydraulic diameter.

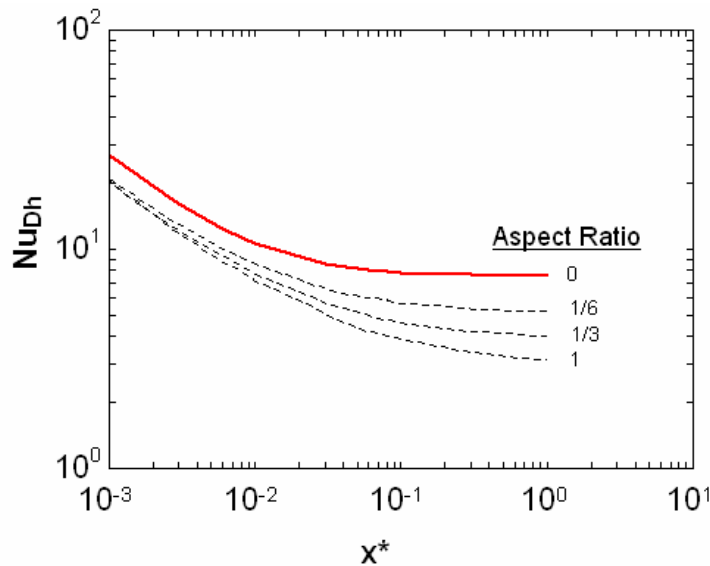


Figure 1. Nusselt number dependence on flow length and aspect ratio.

The Stephan correlation (zero aspect ratio channel) is shown by the solid line and represents an upper bound for all channel flows. The dashed lines below the Stephan line are points calculated using the 3D channel flow correlation for correlation with 3 aspect ratios ranging from 1 to 1/6. As aspect ratio gets smaller, the 3D channel flow heat transfer coefficient approaches the Stephan correlation as expected. All aspect ratios (including the zero aspect ratio Stephan curve) approach the fully developed flow result as x^* becomes larger. The larger the channel aspect ratio, the lower the heat transfer coefficient – an effect that is accentuated for large x^* . The 3D channel flow heat transfer correlation appears above as Equation 7.

4. 3D CHANNEL DARCY FRICTION FACTOR

Equation 8 is the 3D channel Darcy friction factor correlation. It shows how the 2D developing flow equation was modified. Firstly Shah and London's (1978) multiplicative polynomial for the fully developed case was added. Secondly, 8 empirical parameters were inserted into the terms characterizing developing flow. As in the heat transfer case, the parameters were estimated using a least-squares approach. The curve fit was weighted in an attempt to achieve a more uniform distribution in deviations from results by Curr *et al.* (1972) and flat plate numbers. The curve was fit to points taken from numerical solutions presented graphically by Curr *et al.* (1972) for $0.002 \leq x^+ \leq 0.1$, who reported that his results compared well to experimental data taken by Beavers *et al.* (1970). Equation 8 is formulated to ensure that the physically known limits of 2-D flow and fully developed 3D flow are approached as $\alpha \rightarrow 0$ and $x^+ \rightarrow \infty$.

$$f_{3D} \text{Re}_{Dh} = 4 \cdot \left[\frac{3.44 + E_1 \cdot \alpha^{E_2}}{(x^+)^{1/2}} + \frac{24 + \frac{0.674 + F_1 \cdot \alpha^{F_2}}{4x^+} - \frac{3.44 + G_1 \cdot \alpha^{G_2}}{(x^+)^{1/2}}}{1 + (0.000029 + H_1 \cdot \alpha^{H_2})(x^+)^{-2}} \right] \times (1 - 1.3553\alpha + 4.97\alpha^2 - 5.119\alpha^3 + 2.702\alpha^4 - 0.548\alpha^5) \quad (8)$$

where

$E_1=2.359$	$E_2=0.5553$	$F_1=3.434$	$F_2=4.001$
$G_1=3.42$	$G_2=3.204$	$H_1=0.001163$	$H_2=10000$

The flat plate limit was included in the heat transfer correlation, and the 2D friction factor correlation (Equation 4) was used as the limit for small x^+ (below 0.002) for all aspect ratios. The curve fit of Curr's (1972) results included a range of x^+ values from 0.1 to 0.002 for aspect ratios of 0.2, 0.5, and 1. At the minimum x^+ value of 0.002 the friction factor-Reynolds number product had approached the same value for all aspect ratios. This indicates that the flat plate situation has been reached near the leading edge because the boundary layer interactions at the corners have not yet developed to a point where they have a significant effect on friction. The accuracy of the 3D channel friction factor is believed to be better with small aspect ratios and large x^+ values due to the constraints imposed by Equations 4 and 6.

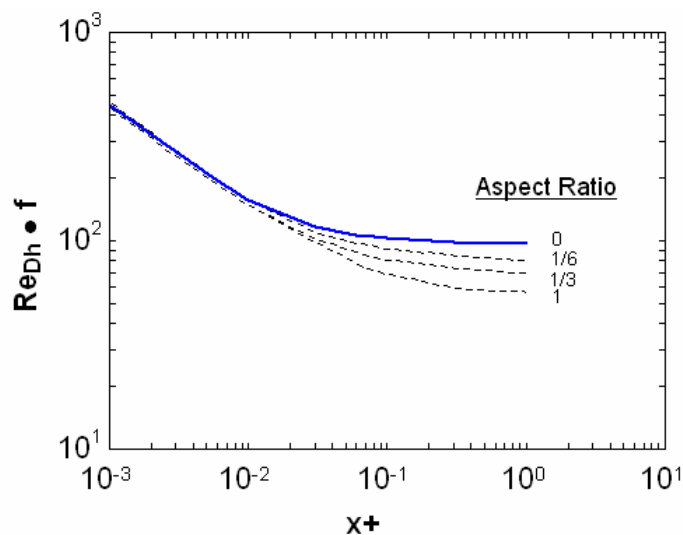


Figure 2. Reynolds number – Darcy friction factor product in rectangular ducts

Figure 2 to the left shows the product of Reynolds number and friction factor predicted by the 3D channel friction correlation compared to the 2D duct. The 3D channel correlation is shown using dashed lines for 3 aspect ratios ranging from 1 to 1/6. The flat duct correlation is shown using a solid line. The product of Reynolds number and friction factor is largest at small x^+ , reflecting the thinner boundary layer. Smaller aspect ratios produce higher friction factors due to larger velocity gradient at the wall in fully developed flow. Near the leading edge of the fins (small x^+) aspect ratio has little to no effect on friction because the boundary layers have not yet grown thick enough to interact.

5. RESULTS

Tables 2 and 3 show the percent deviations between the correlations developed here, and the tabulated analytical results of Wibulswas (1966) and the numerical results of Curr *et al.* (1972). Recall that their results were reported to lie within a few percent of experimental data. These Tables quantify the additional uncertainty attributable to our curve fits that cover the broadest parameter range and converge to known physical limits at the maximum and minimum heat exchanger depths and at an aspect ratio of zero. The last two x^* values in Table 2 extend beyond Wibulswas' (1966) results. These are flat plate values where the accuracy of the 3D channel heat transfer correlation is compared the heat transfer from a flat plate. The last three x^+ values in Table 3 extend beyond Curr's (1972) results. These are flat plate values where the accuracy of the 3D channel friction factor correlation is compared to the friction factor of the 2D duct (Equation 4). At this low x^+ a flat plate and a channel of any aspect ratio will have the same friction factor.

Table 2. Percentage deviations: 3D channel heat transfer

1/x*	α				
	1	0.5	1/3	0.25	1/6
10	-1.9	-1.8	0.2	0.9	1.9
20	-3.3	-2.8	0.3	1.3	2.3
30	-3.2	-2.5	0	1.7	2.7
40	-2.3	-2.1	0.2	1.9	2.9
50	-1.6	-1.7	0.5	1.5	3
60	-0.9	-1.4	0.3	1.6	2.9
80	-0.4	-1.4	0.4	1.2	2.3
100	0.5	-1.1	0.2	1	2.1
120	0.9	-0.8	0.3	0.6	1.7
140	1.5	-0.6	0	0.4	1.5
160	1.9	-0.3	-0.1	0.3	1
180	2.2	0	0	0.1	0.7
200	2.6	0.1	-0.2	-0.1	0.5
220	2.6	0	-0.3	-0.4	0.1
2115	-4.4	-4.4	-4.6	-4.8	-5.1
6667	0.9	3.1	3.3	3.2	2.7

The accuracy of Wibulswas' calculations were within a couple percent for Graetz numbers (Gz) less than 70 (Graetz number = $1/x^*$). For larger Graetz numbers the heat transfer coefficient approaches that of a flat plate. Physically, the heat transfer from a 3D channel must lie between that of a flat plate and the 2D Stephan correlation. No experimental measurements were taken. The maximum error in the Nusselt number curve fit is $\pm 5\%$. The RMS error of the curve fit is 1.5% and the individual errors appear in Table 2. Negative values in the table indicate an underestimation by the curve fit, most prevalent at aspect ratios of 1 and 0.5. The only limit on the 3D channel heat transfer correlation is that the nondimensional depth x^* be greater than $1/6667$.

Table 3. Percentage deviations: 3D channel friction

1/x+	α		
	1	0.5	0.2
10	-0.9	2.6	3.5
14	0.4	0	5.2
17	-0.6	-1.6	5.7
20	-2.6	-0.8	4.3
25	0.5	0.2	4.2
33	2.5	-2.4	2.5
50	1.1	-0.5	2.3
67	-3.1	-3.6	0.2
100	-2	-2.7	1.2
125	-3.5	-3.7	-0.6
143	-1.9	-1.7	0.7
167	-2.6	-2.2	1.4
200	-3.4	-2.7	1.6
250	-2.1	-1.3	1.2
333	4.7	5.1	1.8
500	-2.9	-3.7	1.7
1000	-2.2	-4.9	1.2
1854	-1.1	-4.9	1.5
5247	-0.3	-4.9	1.7

Numerical data from Curr *et al.* (1972) was used to fit 8 constants included in the 3D correlation. The 3D channel friction factor correlation (Equation 8) was found to approximate Curr's data with a RMS error of 2.7% and a maximum error of $\pm 6\%$ at an aspect ratio of 0.2 and an x^+ of $1/17$. The only limit on the 3D channel friction factor correlation is that the nondimensional depth x^+ be greater than $1/5247$.

6. CONCLUSIONS

Semi-empirical correlations for friction factors and Nusselt numbers in 3D rectangular channel airflow were presented. These correlations make use of physically known channel limits to facilitate extrapolation to any scale. The curves were fit to analytical and numerical results for 2D and 3D channels that had previously been found to approximate experimental data within a few percent. The RMS errors of the curve fits developed here are of comparable magnitude. The resulting expressions span the entire parameter space for any rectangular channel geometry except a very small neighborhood of the leading edge.

NOMENCLATURE

A	Channel cross section area	(m ²)	Subscripts
D _h	Hydraulic diameter = 4A/P	(m)	FD fully developed
f	Darcy friction factor	(-)	rect rectangular
Gz	Graetz Number = 1/x*	(-)	
k	Thermal conductivity	(W/mK)	Superscripts
Nu	Nusselt number = hD _h /k	(-)	* dimensionless
P	Wetted perimeter	(m)	+ dimensionless
Pr	Prandtl number	(-)	
Re	Reynolds number = VD _h /ν	(-)	
x	Channel depth	(m)	
α	Aspect ratio	(-)	

REFERENCES

1. Beavers G.S., Sparrow E.M., and Magnuson R.A., 1970. Experiments on hydrodynamically developing flow in rectangular ducts of arbitrary aspect ratio., *Int. J. Heat Mass Transfer* 13 (1970) 689 – 703.
2. Curr R. M., Sharma D., and Tatchell D.G. 1972. “Numerical predictions of some three-dimensional boundary layers in ducts”, *Computer Methods in Applied Mechanics and Engineering* 1, pp 143-158, 1972.
3. Muzychka Y.S., and Yovanovich M. M. 2004. Laminar forced convection heat transfer in the combined entry region of non-circular ducts. *J. of Heat Transfer* 126 54 – 61.
4. Shah R. K. and London A. L. 1978. “*Laminar Flow Forced Convection in Ducts*”, Supplement 1 to *Advances in Heat Transfer*, Academic, New York, 1978.
5. Stephan K., 1959. Warmeübergang und druckabfall bei nicht ausgebildeter Laminarströmung in Röhren und in ebenen Spalten, *Chem.-Ing.-Tech.*, Vol 31, pp. 773-778, 1959.
6. Wang C.-C., Lee C.-J., Chang C.-T., and Lin S.-P. 1999. Heat transfer and friction correlation for compact louvered fin-and-tube heat exchangers. *Int. J. Heat Mass Transfer* 42 1945 – 1956.
7. Wibulswas, P. 1966. “*Laminar Flow Heat Transfer in Non-Circular Ducts*”, Ph.D. Thesis, London Univ., London, 1966.

ACKNOWLEDGEMENT

This work was supported by the member companies of the Air Conditioning and Refrigeration Center at the University of Illinois at Urbana-Champaign.